



Contents lists available at ScienceDirect

# Radiotherapy and Oncology

journal homepage: [www.thegreenjournal.com](http://www.thegreenjournal.com)

First in Human

## First clinical real-time motion-including tumor dose reconstruction during radiotherapy delivery



Simon Skouboe<sup>a,\*</sup>, Thomas Ravkilde<sup>b</sup>, Jenny Bertholet<sup>c</sup>, Rune Hansen<sup>b</sup>, Esben Schjødt Worm<sup>b</sup>, Casper Gammelmark Muurholm<sup>a</sup>, Britta Weber<sup>a,d</sup>, Morten Høyer<sup>d</sup>, Per Rugaard Poulsen<sup>a,d</sup>

<sup>a</sup> Department of Oncology, Aarhus University Hospital; <sup>b</sup> Department of Medical Physics, Aarhus University Hospital, Denmark; <sup>c</sup> Joint Department of Physics, The Institute of Cancer Research and the Royal Marsden Hospital NHS Foundation Trust, London, UK; and <sup>d</sup> Danish Center for Particle Therapy, Aarhus University Hospital, Denmark

### ARTICLE INFO

#### Article history:

Received 21 February 2019

Received in revised form 25 June 2019

Accepted 4 July 2019

Available online 17 August 2019

#### Keywords:

Real-time dose calculation

Tumor motion

Motion management

### ABSTRACT

**Purpose:** To clinically implement and characterize real-time motion-including tumor dose reconstruction during radiotherapy delivery.

**Methods:** Seven patients with 2–3 fiducial markers implanted near liver tumors received stereotactic body radiotherapy on a conventional linear accelerator. The 3D marker motion during a setup CBCT scan was determined online from the CBCT projections and used to generate a correlation model between tumor and external marker block motion. During treatment, the correlation model was updated by kV imaging every three seconds and used for real-time tumor localization. Using streamed accelerator parameters and tumor positions, in-house developed software, DoseTracker, calculated the dose to the moving tumor in real-time assuming water density in the patient. Post-treatment, the real-time tumor localization was validated by comparison with independent marker segmentations and 3D motion estimations. Dose reconstruction was validated by comparison with treatment planning system (TPS) calculations that modeled motion as isocenter shifts and used both actual CT densities and water densities.

**Results:** The real-time estimated tumor position had a mean 3D root-mean-square error of 1.7 mm (range: 0.9–2.6 mm). The motion-induced reduction in the minimum dose to 95% of the clinical target volume (CTV D95) per fraction was up to 12.3%-points. It was estimated in real-time by DoseTracker during patient treatment with a root-mean-square difference relative to the TPS of 1.3%-points (TPS CT) and 1.0%-points (TPS water).

**Conclusions:** The world's first clinical real-time motion-including tumor dose reconstruction during radiotherapy was demonstrated. This marks an important milestone for real-time in-treatment quality assurance and paves the way for real-time dose-guided treatment adaptation.

© 2019 Elsevier B.V. All rights reserved. Radiotherapy and Oncology 139 (2019) 66–71

The utility of stereotactic body radiotherapy (SBRT) is clearly increasing [1]. High accuracy at each individual fraction is essential, but also challenged by intrafraction motion and anatomical changes [2–5]. For liver SBRT, studies on dose reconstruction has demonstrated that motion can substantially deteriorate the tumor dose [6–8]. These motion-including dose calculations were performed post-treatment with no possibility to intervene in case of unacceptable dose errors. Real-time motion-including dose reconstruction was recently demonstrated in simulated treatments [9–11] and phantom treatments [12], but it has not yet been applied during actual patient treatments. Here, we present the world's first clinical real-time motion-including tumor dose reconstruction during radiotherapy delivery.

### Methods

Real-time motion-including tumor dose reconstruction was performed with the in-house developed program DoseTracker [12] at a total of ten treatment fractions for seven patients treated with SBRT for primary hepatocellular carcinoma ( $n = 1$ ), cholangiocarcinoma ( $n = 1$ ), or one ( $n = 3$ ) or two ( $n = 2$ ) liver metastases. Each patient had 2–3 fiducial markers implanted near the lesion (s). A planning target volume (PTV) was constructed by expanding the clinical target volume (CTV) with 5 mm in the left–right (LR) and anterior–posterior (AP) directions and 10 mm in the cranio-caudal (CC) direction. The prescribed mean CTV dose was 48 Gy in three or six fractions (primary tumors) or 56.25 Gy in three fractions (metastases). A treatment planning system (TPS, Eclipse 13.7, Varian Medical Systems, Palo Alto, CA) was used to design a three-arc volumetric modulated arc therapy (VMAT) plan that covered the CTV with 95% and the PTV with 67% of the prescribed dose.

\* Corresponding author at: Department of Oncology, Aarhus University Hospital, Palle Juul-Jensens Boulevard 99, 8200 Aarhus N, Denmark.

E-mail address: [simsko@rm.dk](mailto:simsko@rm.dk) (S. Skouboe).

Abdominal compression was used for all but one patient (due to discomfort). Patient setup was based on a cone-beam CT (CBCT) scan with match on the gold markers.

As illustrated in Fig. 1, the dose reconstruction relied on real-time tumor motion monitoring by an in-house developed method of Combined Optical and Sparse Monoscopic Imaging with

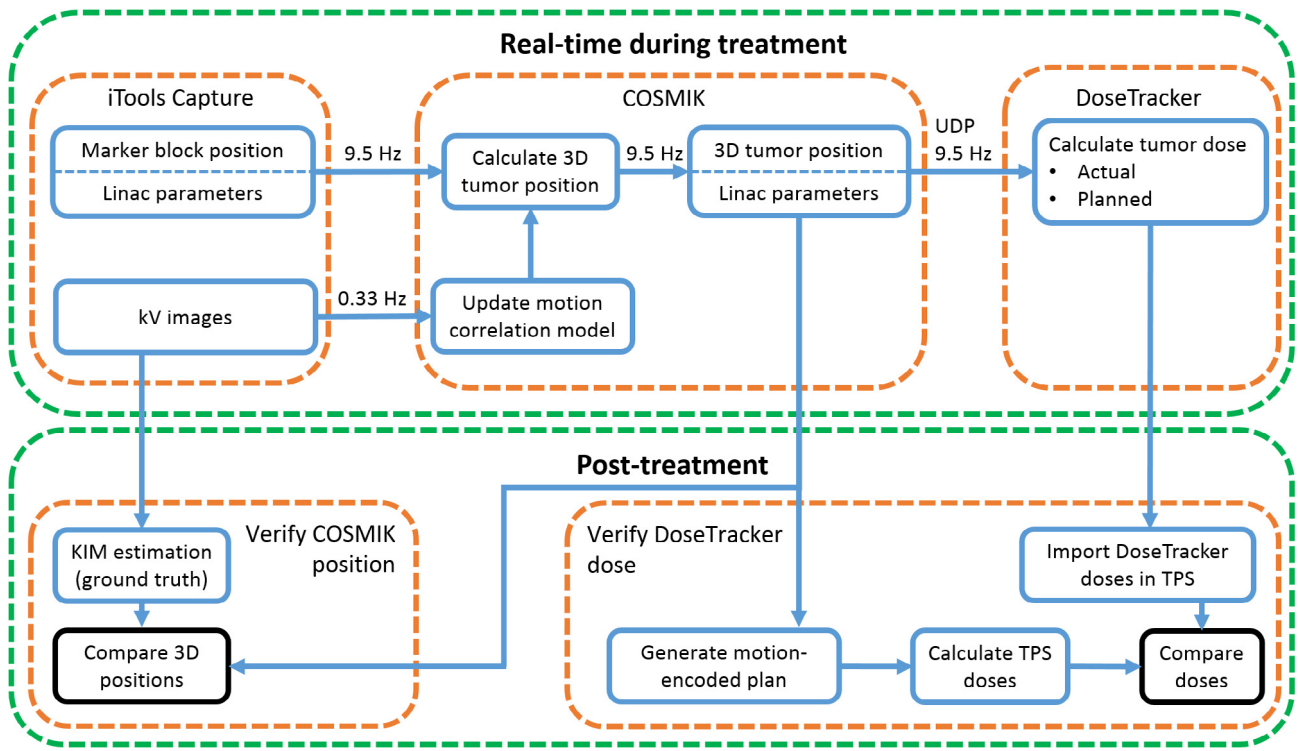


**Fig. 1.** Workflow of the study. See the text for details. During treatment delivery, the tumor position was estimated in real time by the COSMIK method and streamed along with linac parameters to DoseTracker, which calculated both the actual (motion-including) and planned (static) tumor dose in real-time (top). Post-treatment verification of the real-time COSMIK localization (bottom left) and DoseTracker dose (bottom right).

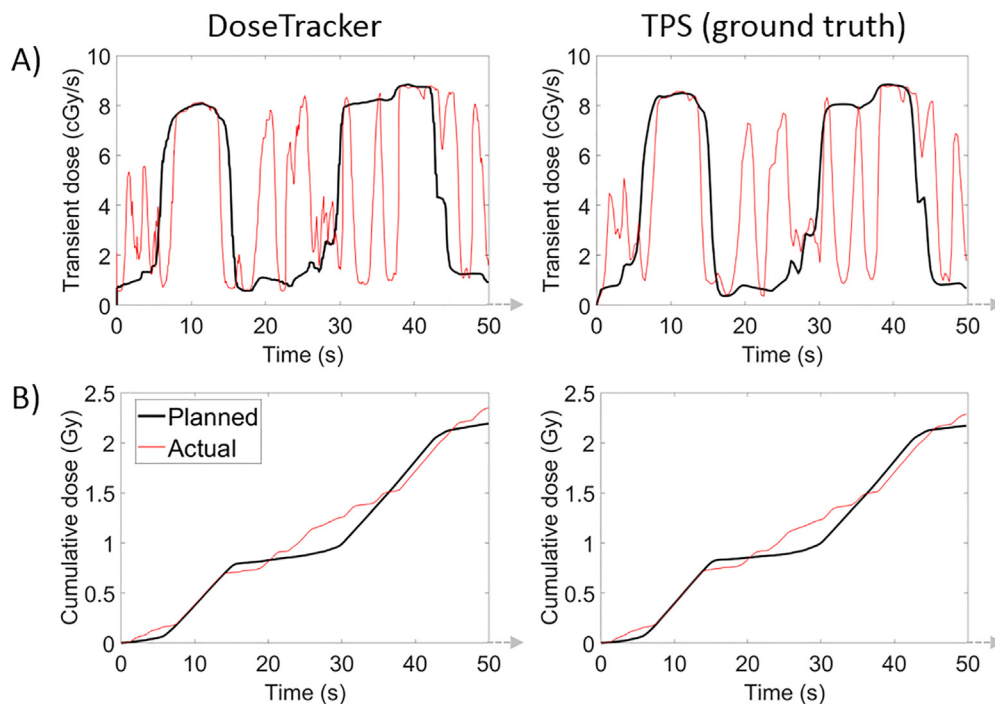


**Fig. 2.** Time-resolved doses to a point. Actual (red, thin) and planned (black, thick) (A) transient and (B) cumulative dose during the first 50 s of a fraction in a point in the cranial part of the tumor (indicated by the white dot in Fig. 4) as calculated in real-time by DoseTracker (left) and post-treatment by the treatment planning system (TPS, CT tissue densities) (right). Differences between DoseTracker and the TPS can be seen in Fig. 3. (For interpretation of the references to colour in this figure legend, the reader is referred to the web version of this article.)

Kilovoltage X-rays (COSMIK [13]). At each session, the COSMIK program streamed the position of an external marker block on the patient's abdomen and all kV images from the linac via a research frame grabber system (iTools Capture, Varian Medical Systems). Before treatment onset, COSMIK segmented the marker positions in all CBCT projections, estimated the 3D marker trajectories using a probability-based method and used this to establish a correlation model between the external marker block motion and the internal three-dimensional (3D) motion of each implanted marker [13]. This did not delay treatment start, since it was completed during the manual CBCT match and couch correction procedures. During treatment delivery, COSMIK continuously estimated the internal 3D marker position in real time from the marker block motion. The correlation model was updated with automatic marker segmentation from kV images acquired during beam pauses every 3 s [13]. Marker segmentations with a low confidence were rejected and not used for model update [13]. COSMIK assumed the same tumor position relative to the markers as at treatment planning and broadcasted the tumor position and all accelerator parameters to DoseTracker at 9.5 Hz as Unified Data Protocol (UDP) messages. In a continuous loop, DoseTracker used a simplified pencil beam algorithm [14] that assumed water density of the patient to calculate the dose in real-time to the same calculation points as used by the TPS within the PTV. The dose was first calculated in the isocenter plane by convolving a pencil beam kernel with a field intensity function (defined by the MLC aperture and jaws), and then scaled in depth to all calculation points [14]. At each calculation time, the dose increment in each point was calculated both as actually delivered with the real-time estimated tumor position and as planned without motion. The calculation of actually delivered dose used the streamed actual accelerator parameters, while the calculation of the planned dose used accelerator parameters from the treatment plan.

Post-treatment, the accuracy of the real-time marker localization and dose reconstruction was estimated by comparison with more accurate calculations (Fig. 1, bottom). The markers were segmented in all intra-treatment kV images using cylindrical marker templates [15] and manually corrected if the segmentation error exceeded two pixels as deemed by visual inspection. The 3D marker positions for each kV image were estimated by the probability-based method used for Kilovoltage Intrafraction Monitoring (KIM) [16], reported to have sub-millimeter accuracy [17]. Using these 3D positions as ground truth, the root-mean-square (RMS) localization error of COSMIK at the time of kV imaging was calculated for the marker constellation centroid.

A ground truth tumor dose with the real-time estimated tumor motion was obtained by generating a plan that emulated motion as multiple isocenter shifts and calculating this motion-encoded plan in the TPS [18] using Acuros XB 13.7.14 (Varian Medical Systems). The TPS calculations were performed both with the actual CT tissue density and with water density to investigate the impact of the water density assumption of DoseTracker. The real-time calculated doses from DoseTracker were imported into the TPS and compared with the ground truth dose in terms of the difference between the planned static CTV dose and the actual CTV dose with motion. The motion-induced reductions in the mean CTV dose ( $\Delta D_{\text{mean}}$ ) and minimum doses to 95% and 98% of the CTV ( $\Delta D_{95}$  and  $\Delta D_{98}$ ) were compared between DoseTracker and the TPS. Furthermore, the time-resolved dose in a selected calculation point in the tumor 1.2 cm cranially from the isocenter was compared between DoseTracker and the TPS for one fraction. Here, the time resolved dose in the TPS was obtained by accumulating the dose in each 0.5° gantry rotation interval during the VMAT delivery [19], which corresponded to a time resolution of approximately 0.6 s. For each fraction, all cumulative point doses of DoseTracker were compared with the corresponding TPS CT doses for both the actual motion-

including dose and the planned dose. The mean and the standard deviation of the dose error of DoseTracker were calculated and used to represent the systematic and random dose reconstruction error of DoseTracker at a fraction.

## Results

In the patient recruitment period, real-time dose reconstruction was attempted for twenty treatment fractions for eight consecutive liver SBRT patients. The real-time dose reconstruction was,

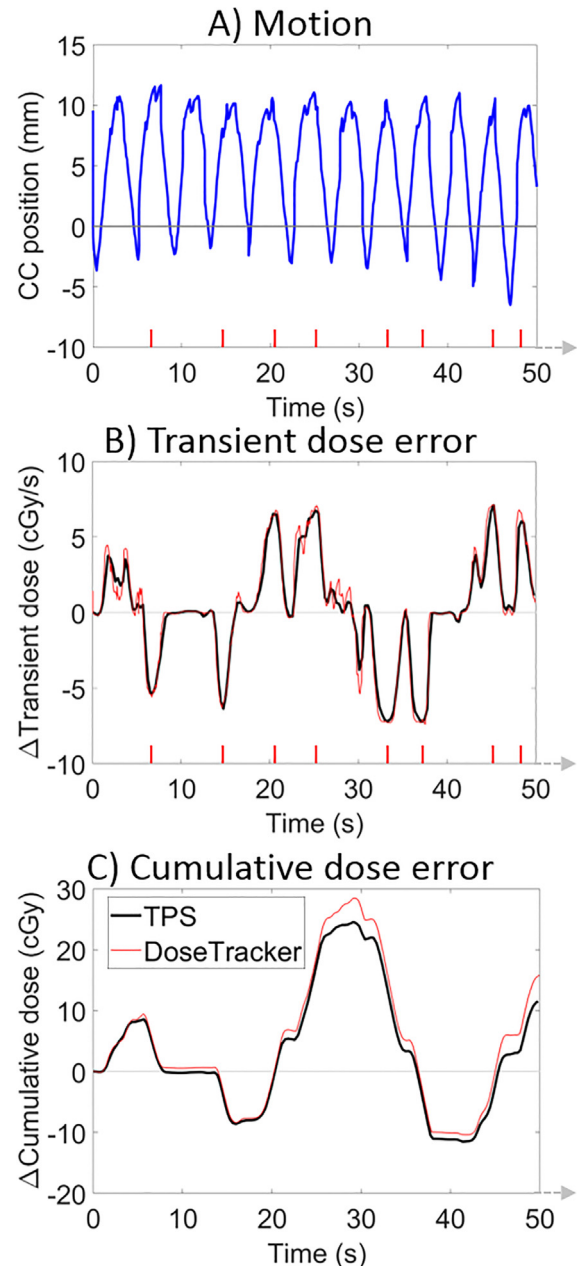


**Fig. 3.** Tumor motion and motion-induced dose error in a point. (A) Tumor motion in the cranio-caudal direction during the first 50 s of a fraction. (B) Transient dose error and (C) cumulative dose error in the point shown in Fig. 2 (white dot in Fig. 4) as calculated in real time by DoseTracker (red, thin lines) and post-treatment by the treatment planning system (TPS CT tissue density) (black, thick lines). Absolute transient dose errors larger than 5 cGy/s were associated with large tumor excursions as indicated with ticks on the time axis. (For interpretation of the references to colour in this figure legend, the reader is referred to the web version of this article.)

however, only successful for the ten included fractions (covering seven patients). The failed real-time dose reconstructions were due to user preparation errors ( $n = 2$ ), system crash ( $n = 1$ ), communication failures between COSMIK and DoseTracker ( $n = 5$ ) or inactivated COSMIK correlation model updates ( $n = 2$ ).

On average, 169 intra-treatment kV images (range: 82–201) were acquired at each fraction. The treatment was in mean delayed by 0.5 s per image acquisition as the gantry was rotated back in order to resume the VMAT treatment. The COSMIK program performed real-time marker segmentation in 91.5% of the intra-treatment kV images (range: 58–100%). Post-treatment segmentation in all images showed that the mean (range) RMS localization error of COSMIK at a fraction was 0.8 mm (0.2–2.1 mm) (LR), 1.1 mm (0.6–2.0 mm) (CC), 0.9 mm (0.3–1.6 mm) (AP), and 1.7 mm (0.9–2.6 mm) (3D).

The mean PTV volume was 59.5 cm<sup>3</sup> (range: 31.4–84.4 cm<sup>3</sup>) with 3197 (range: 1694–4520) calculation points in a regular grid with 2.5 mm (LR, AP) and 3 mm (CC) spacing. DoseTracker was allowed to average over UDP messages spanning up to 500 ms [12], but in general reconstructed the actual and planned dose increments in all calculation points at the same 9.5 Hz rate as the UDP messages from COSMIK: 96.8%, 1.8% and 1.4% of the dose calculations spanned one, two and more UDP messages, respectively. The real-time calculated time-resolved actual and planned dose in the single test point was very similar to the ground truth TPS CT

dose (Fig. 2). Substantial dose errors, i.e. deviations between the actual and planned transient dose in the point, were associated with larger tumor excursions caused by respiration (Fig. 3). Despite its simplified algorithm, DoseTracker reconstructed dose errors well for the test point (Fig. 3B–C). Comparing the cumulative dose of all calculation points, the mean (systematic) error in the reconstructed DoseTracker dose at a fraction was on average 3.2%-points (range 0.4–8.3%-points). DoseTracker thus tended to over-estimate the absolute dose. However, the systematic mean dose reconstruction error at a fraction was often quite similar for the actual dose and the planned dose with a mean (maximum) absolute difference of 0.8%-points (2.9%-points). Therefore, the systematic error of DoseTracker tended to cancel out when the motion-induced error was calculated as the difference between the actual and the planned dose. The standard deviation (random) dose error of DoseTracker at a fraction was on average 3.2%-points (range: 2.0–5.3% points). DoseTracker calculated CTV  $D_{\text{mean}}$  with a mean error of 4.0%-points (range –2.8 to 9.9%-points, RMS error: 5.3%-points) for the actual motion-including dose and 4.4%-points (range –2.4 to 9.8%-points, RMS error: 5.8%-points) for the planned static dose. Fig. 4 shows the reconstructed cumulative tumor doses at a fraction with CTV  $D_{\text{mean}}$  of 97.2% (actual) and 101.8% (planned) in the DoseTracker calculation and 95.5% (actual) and 100% (planned) in the ground truth TPS CT calculation. Note that the dose color display for DoseTracker has been scaled to the DoseTracker mean

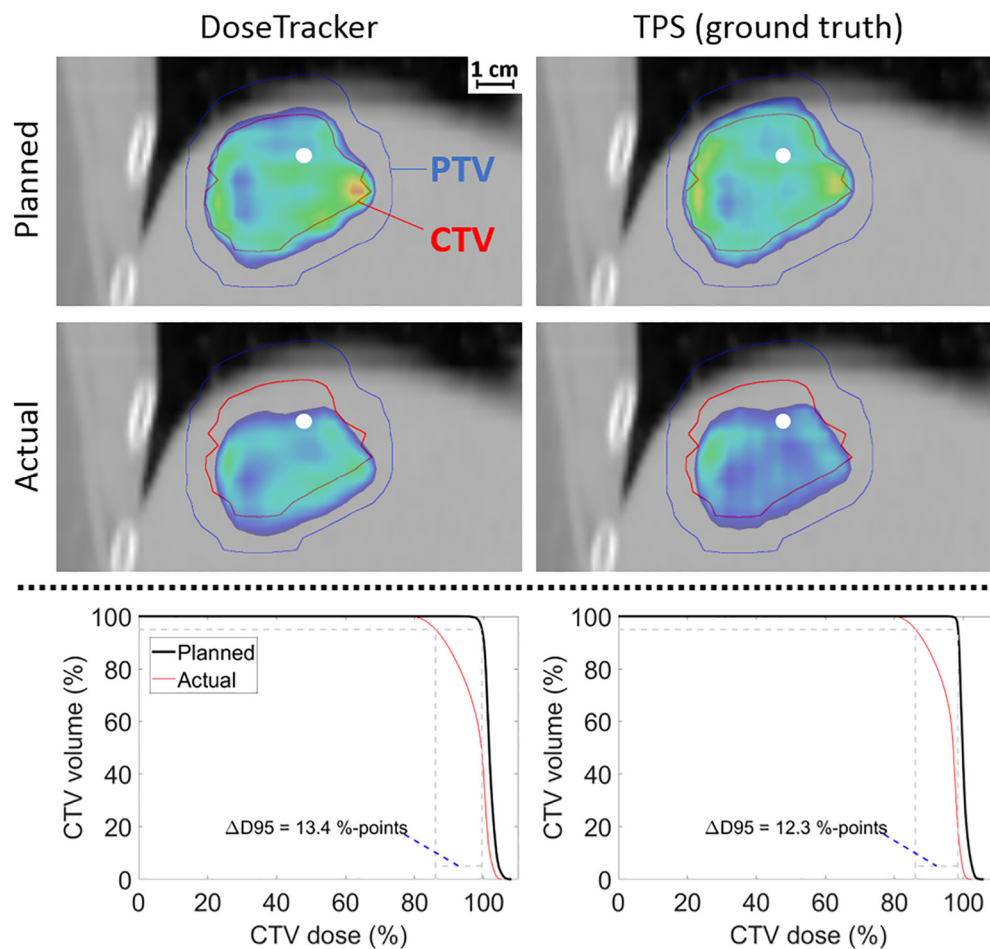


**Fig. 4.** Final tumor dose for a fraction. Top: Planned and actual dose distributions in the coronal slice through the isocenter for DoseTracker (left) and the treatment planning system (TPS CT density) (right) after delivery of the whole fraction. The dose color wash range is 95–107% of the mean CTV dose as calculated by DoseTracker and the TPS, respectively. Figs. 2 and 3 show the time-resolved dose in the point indicated by a white dot. Bottom: Dose volume histograms for the CTV as planned (black, thick) and actually delivered (red, thin) for the DoseTracker (left) and TPS (right) doses. The motion-induced reduction in CTV  $D_{95}$  is indicated. (For interpretation of the references to colour in this figure legend, the reader is referred to the web version of this article.)

CTV dose in the figure. Since DoseTracker over-estimated both the actual and planned dose by approximately the same amount, it gave good estimations of the motion-induced  $\Delta D_{\text{mean}}$  (4.5%-points vs 4.5 %-points with the TPS),  $\Delta D_{95}$  (13.4%-points vs 12.3%-points) and  $\Delta D_{98}$  (15.3%-points vs 14.3%-points).

The motion resulted in CTV dose reductions of up to 4.5%-points ( $D_{\text{mean}}$ ), 12.3%-points ( $D_{95}$ ), and 14.3%-points ( $D_{98}$ ) as calculated by the TPS (CT densities). The motion-induced reduction in CTV dose coverage reconstructed in real-time by DoseTracker agreed well with the TPS with RMS differences over all fractions and tumors of 0.9%-points ( $\Delta D_{\text{mean}}$ ), 1.3%-points ( $\Delta D_{95}$ ) and 1.5%-points ( $\Delta D_{98}$ ) (Fig. 5, top). Outliers were mainly caused by the water density approximation in the current version of DoseTracker as seen by a substantially better agreement between DoseTracker and TPS water density calculations (Fig. 5, bottom).

## Discussion

In this study, real-time motion-including tumor dose reconstruction during patient treatments was demonstrated for the first time by combining in-house developed real-time methods for tumor motion monitoring and dose calculation. Sufficiently fast dose reconstruction for real-time use was obtained by a simplified dose algorithm that nevertheless estimated the motion-induced tumor dose reduction accurately. It should be noted that the motion monitoring and dose calculation only rely on standard equipment on a conventional linear accelerator, making the methods portable to most linear accelerators. Although this first demonstration focused on the tumor dose and assumed rigid

motion, the real-time dose reconstruction could also be performed for organs-at-risk and include more complex motion such as rotations [20] and deformations if such motion were available in real time, e.g. by MR imaging.

While DoseTracker modeled motion as rigid tumor shifts inside the patient, the TPS in effect shifted the entire patient in discretized steps of 1.5 mm [18]. This difference between methods is only expected to give small tumor dose differences, which justifies the use of the TPS isocenter shift method as ground truth in this study. Since the goal was to quantify the dose reconstruction accuracy, it should be acceptable to use the slightly imprecise real-time COSMIK localization data as tumor motion in the comparisons between DoseTracker and TPS. DoseTracker estimated the absolute dose relatively poorly with a CTV  $D_{\text{mean}}$  RMS error of 5.8%-points. We ascribe the dose overestimation to an overly simple scaling of the dose with the MLC aperture, where DoseTracker uses an equivalent square field that has the same area as the total area of the MLC aperture. However, the reduction in CTV dose coverage caused by motion was reconstructed more accurately with RMS errors of 0.9–1.5%-points for CTV  $\Delta D_{\text{mean}}$ ,  $\Delta D_{95}$  and  $\Delta D_{98}$  since errors present in both the motion dose and static dose tended to cancel out when the two doses were subtracted. The better agreement of DoseTracker with TPS water calculations than with TPS CT calculations (Fig. 5) suggests that tissue density modeling could improve the accuracy of DoseTracker substantially. Tissue density modeling will most likely also be required for application of DoseTracker in the lung. Adding this will increase the computation time, but we do not anticipate major issues. Other potential improvements of DoseTracker include

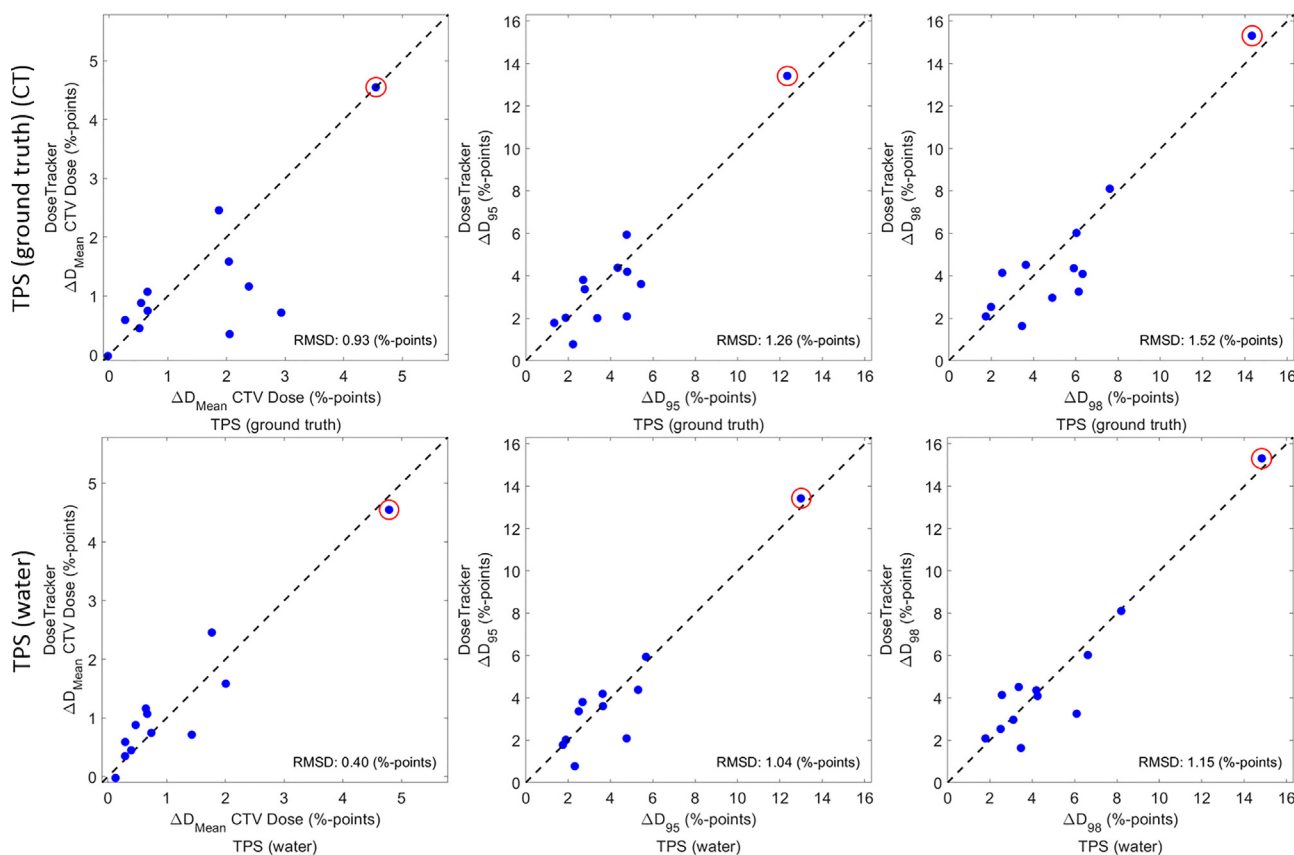


**Fig. 5.** Reduction in tumor dose coverage. Motion-induced CTV dose reduction for all tumors and fractions as calculated by DoseTracker plotted against the treatment planning system (TPS) using both CT (top) and water densities (bottom). The graphs show the reduction in CTV mean dose ( $\Delta D_{\text{Mean}}$ ) (left),  $D_{95}$  ( $\Delta D_{95}$ ) (middle), and  $D_{98}$  ( $\Delta D_{98}$ ) (right). The red circles indicate the case used in examples in Figs. 2–4. The unity line indicates perfect agreement of dose error reconstruction. The numbers indicate the root-mean-square difference between DoseTracker and the TPS. (For interpretation of the references to colour in this figure legend, the reader is referred to the web version of this article.)

modeling of skin obliquity and off-axis factors. Furthermore, the robustness of the integrated system with COSMIK motion monitoring and DoseTracker dose reconstruction must be improved as five out of twenty attempts of real-time dose reconstruction failed due to communication errors between COSMIK and DoseTracker (while user errors or hardware malfunction caused five other failures).

Other researchers have pursued real-time treatment validation [9–11,21,22]. However, these studies either disregarded motion [21,22] or they were used pre-clinically without any evaluation until the end of the treatment fraction [9–11]. All of these studies additionally relied on a number of pre-calculations, limiting their applicability to a certain range of treatment scenarios. In contrast, DoseTracker calculates doses in completeness at treatment without the limitation of pre-calculations within a conceived set of treatment scenarios.

This study was entirely observational without treatment interventions based on the real-time reconstructed tumor dose. However, the dose reconstruction could be used for dose-guided intrafraction treatment adaptation on several time scales ranging from couch corrections between treatment fields to real-time adaptation by gating or tracking [23]. For real-time adaptation, the latency must be low. The latency is here the total time for the dose calculations (typically less than 100 ms; 96.7% of the dose calculations finished before next information in the 9.5 Hz feed arrives) and motion adaptation. Image-guided MLC-tracking has a total latency of about 300 ms [24], but COSMIK is faster since it uses an optical feed [25]. However, for this study we did not log times to analyze this in further detail. Ultimately, real-time adaptation seems realistic. On an interfraction timescale, the indication of large dose errors by DoseTracker could be used to trigger more accurate dose reconstructions and interfraction plan adaptations. In the long term, better knowledge of actually delivered doses may lead to more accurate dose–response relationship models, which currently suffer from a plethora of uncertainties with respect to delivered dose. We believe that DoseTracker could help provide a piece of that puzzle.

In conclusion, the world's first clinical real-time motion-including tumor dose reconstruction during patient treatments was implemented. This marks an important milestone for real-time in-treatment quality assurance and paves the way for intrafraction dose-guided treatment adaptation.

## Declaration of Competing Interest

Aarhus University Hospital received support from Varian Medical Systems related to this study.

## Acknowledgements

This study was supported by The Danish Cancer Society (grants R146-A9373 and R191-A11526), DCCC Radiotherapy (The Danish National Research Center for Radiotherapy) and Varian Medical Systems.

## References

- [1] Koong AC, Tepper JE. Introduction. *Semin Radiat Oncol* 2017;27:189. <https://doi.org/10.1016/j.semradonc.2017.03.005>.
- [2] Worm ES, Hoyer M, Fledelius W, Poulsen PR. Three-dimensional, time-resolved, intrafraction motion monitoring throughout stereotactic liver radiation therapy on a conventional linear accelerator. *Int J Radiat Oncol Biol Phys* 2013;86:190–7. <https://doi.org/10.1016/j.ijrobp.2012.12.017>.
- [3] Worm ES, Hoyer M, Fledelius W, Hansen AT, Poulsen PR. Variations in magnitude and directionality of respiratory target motion throughout full treatment courses of stereotactic body radiotherapy for tumors in the liver. *Acta Oncol (Madr)* 2013. <https://doi.org/10.3109/0284186X.2013.813638>.
- [4] Bertholet J, Worm ES, Fledelius W, Hoyer M, Poulsen PR. Time-resolved intrafraction target translations and rotations during stereotactic liver radiation therapy: implications for marker-based localization accuracy. *Int J Radiat Oncol Biol Phys* 2016. <https://doi.org/10.1016/j.ijrobp.2016.01.033>.
- [5] Poulsen PR, Worm ES, Hansen R, Larsen LP, Grau C, Hoyer M. Respiratory gating based on internal electromagnetic motion monitoring during stereotactic liver radiation therapy: First results. *Acta Oncol (Madr)* 2015;54:1445–52. <https://doi.org/10.3109/0284186X.2015.1062134>.
- [6] Mendez Romero A, Zinkstok RT, Wunderink W, van Os RM, Joosten H, Seppenwoolde Y, et al. Stereotactic body radiation therapy for liver tumors: impact of daily setup corrections and day-to-day anatomic variations on dose in target and organs at risk. *Int J Radiat Oncol Biol Phys* 2009. doi: S0360-3016(08)03916-3 [pii];10.1016/j.ijrobp.2008.12.020.
- [7] Poulsen PR, Worm ES, Petersen JBBB, Grau C, Fledelius W, Hoyer M. Kilovoltage intrafraction motion monitoring and target dose reconstruction for stereotactic volumetric modulated arc therapy of tumors in the liver. *Radiother Oncol* 2014;111:424–30. <https://doi.org/10.1016/j.radonc.2014.05.007>.
- [8] Worm ES, Hoyer M, Hansen R, Larsen LP, Weber B, Grau C, et al. A prospective cohort study of gated stereotactic liver radiation therapy using continuous internal electromagnetic motion monitoring. *Int J Radiat Oncol Biol Phys* 2018. <https://doi.org/10.1016/j.ijrobp.2018.02.010>.
- [9] Fast MF, Kamerling CP, Ziegenhein P, Menten MJ, Bedford JL, Nill S, et al. Assessment of MLC tracking performance during hypofractionated prostate radiotherapy using real-time dose reconstruction. *Phys Med Biol* 2016;61:1546–62. <https://doi.org/10.1088/0031-9155/61/4/1546>.
- [10] Kamerling CP, Fast MF, Ziegenhein P, Menten MJ, Nill S, Oelfke U. Online dose reconstruction for tracked volumetric arc therapy: real-time implementation and offline quality assurance for prostate SBRT: real-time. *Med Phys* 2017;44:5997–6007. <https://doi.org/10.1002/mp.12522>.
- [11] Kamerling CP, Fast MF, Ziegenhein P, Menten MJ, Nill S, Oelfke U. Real-time 4D dose reconstruction for tracked dynamic MLC deliveries for lung SBRT. *Med Phys* 2016;43. <https://doi.org/10.1118/1.4965045>.
- [12] Ravkilde T, Skouboe S, Hansen R, Worm E, Poulsen PR, Ravkilde T. First online real-time evaluation of motion-induced 4D dose errors during radiotherapy delivery. *Med Phys* 2018;45:3893–903. <https://doi.org/10.1002/mp.13037>.
- [13] Bertholet J, Toftegaard J, Hansen R, Worm ES, Wan H, Parikh PJ, et al. Automatic online and real-time tumour motion monitoring during stereotactic liver treatments on a conventional linac by combined optical and sparse monoscopic imaging with kilovoltage X-rays (COSMIK). *Phys Med Biol* 2018. <https://doi.org/10.1088/1361-6560/aaae8b>.
- [14] Ravkilde T, Keall PJ, Grau C, Hoyer M, Poulsen PR. Fast motion-including dose error reconstruction for VMAT with and without MLC tracking. *Phys Med Biol* 2014;59:7279–96. <https://doi.org/10.1088/0031-9155/59/23/7279>.
- [15] Fledelius W, Worm E, Elstrøm UV, Petersen JB, Grau C, Hoyer M, et al. Robust automatic segmentation of multiple implanted cylindrical gold fiducial markers in cone-beam CT projections. *Med Phys* 2011;38:6351–61. <https://doi.org/10.1118/1.3658566>.
- [16] Keall PJ, Aun Ng J, O'Brien R, Colvill E, Huang C-YY, Rugaard Poulsen P, et al. The first clinical treatment with kilovoltage intrafraction monitoring (KIM): a real-time image guidance method. *Med Phys* 2015;42:354–8. <https://doi.org/10.1118/1.4904023>.
- [17] Poulsen PR, Cho B, Keall PJ. A method to estimate mean position, motion magnitude, motion correlation, and trajectory of a tumor from cone-beam CT projections for image-guided radiotherapy. *Int J Radiat Oncol Biol Phys* 2008;72:1587–96. <https://doi.org/10.1016/j.ijrobp.2008.07.037>.
- [18] Poulsen PR, Schmidt ML, Keall P, Worm ES, Fledelius W, Hoffmann L. A method of dose reconstruction for moving targets compatible with dynamic treatments. *Med Phys* 2012;39:6237–46. <https://doi.org/10.1118/1.4754297>.
- [19] Ravkilde T, Keall PJ, Grau C, Hoyer M, Poulsen PR. Time-resolved dose reconstruction by motion encoding of volumetric modulated arc therapy fields delivered with and without dynamic multi-leaf collimator tracking. *Acta Oncol (Madr)* 2013;52:1497–503. <https://doi.org/10.3109/0284186X.2013.818248>.
- [20] Muurholm CG, Ravkilde T, Skouboe S, Eade T, Nguyen DT, Booth J. Dose reconstruction including dynamic six-degree of freedom motion during prostate radiotherapy. *IC3D Dose Conf*, 2019.
- [21] Woodruff HC, Fuangrod T, Van Uytven E, McCurdy BMC, Van Beek T, Bhatia S, et al. First experience with real-time EPID-based delivery verification during IMRT and VMAT sessions. *Int J Radiat Oncol Biol Phys* 2015;93:516–22. <https://doi.org/10.1016/j.ijrobp.2015.07.2271>.
- [22] Spreuw H, Rozendaal R, Olaciregui-Ruiz I, González P, Mans A, Mijneer B, et al. Online 3D EPID-based dose verification: Proof of concept. *Med Phys* 2016;43:3969–74. <https://doi.org/10.1118/1.4952729>.
- [23] Nankali S, Worm ES, Hansen R, Weber B, Hoyer M, Zirk A, et al. Geometric and dosimetric comparison of four intrafraction motion adaptation strategies for stereotactic liver radiotherapy. *Phys Med Biol*, 63. <https://doi.org/10.1088/1361-6560/aacd4a>.
- [24] Poulsen PR, Fledelius W, Cho B, Keall P. Image-based dynamic multileaf collimator tracking of moving targets during intensity-modulated arc therapy. *Int J Radiat Oncol Biol Phys* 2012;83:e265–71. <https://doi.org/10.1016/j.ijrobp.2011.12.053>.
- [25] Dieterich S, Cleary K, D'Souza W, Murphy M, Wong KH, Keall PJ. Locating and targeting moving tumors with radiation beams. *Med Phys* 2008;35:5684–94. <https://doi.org/10.1118/1.3020593>.